12-10-2005

Longitudinal Magnetic Field Changes Accompanying Solar Flares

Jeffrey J. Sudol
West Chester University of Pennsylvania, jsudol@wcupa.edu

J. W. Harvey
National Solar Observatory

The Astrophysical Journal, 635:647–658, 2005 December 10

LONGITUDINAL MAGNETIC FIELD CHANGES ACCOMPANYING SOLAR FLARES

J. J. Sudol and J. W. Harvey
National Solar Observatory, 950 North Cherry Avenue, Tucson, AZ 85719; jsudol@nso.edu, jharvey@nso.edu
Received 2005 May 9; accepted 2005 August 22

ABSTRACT

We have used Global Oscillation Network Group (GONG) magnetograms to characterize the changes in the photospheric longitudinal magnetic field during 15 X-class solar flares. An abrupt, significant, and persistent change in the magnetic field occurred in at least one location within the flaring active region during each event. We have identified a total of 42 sites where such field changes occurred. At 75% of these sites, the magnetic field change occurred in less than 10 minutes. The absolute values of the field changes ranged between 30 and almost 300 G, the median being 90 G. Decreases in the measured field component were twice as frequent as increases. The field changes ranged between 1.4 and 20 times the rms noise of the observations. In all but one equivocal case, the field changes occurred after the start of the flare. In all cases, the field changes were permanent. At least two-thirds of the field changes occurred in the penumbrae of sunspots. During three events for which simultaneous *Transition Region and Coronal Explorer* (*TRACE*) images are available, we have found excellent spatial and temporal correlation between the change in the magnetic field and an increase in brightness of the footpoints of flare ribbons, but not vice versa. Among many possible explanations for the observations, we favor one in which the magnetic field changes result from the penumbral field relaxing upward by reconnecting magnetic fields above the surface. One of the basic assumptions of flare theories is that the photospheric magnetic field does not change significantly during flares. These results suggest that this assumption needs to be re-examined.

Subject headings: Sun: flares — Sun: magnetic fields

1. INTRODUCTION

Understanding solar flares has been a major goal of astrophysics since frequent observations of solar flares became available in the 1920s. Early studies showed that flares were preferentially associated with strong, complicated magnetic fields. Estimates of the energy required to power large flares, together with their association with magnetic fields, led to the conclusion that flares must be electromagnetic in origin. Giovanelli (1948) and Hoyle (1949) developed electric discharge theories that Cowling (1953) later showed to be flawed. Gold & Hoyle (1960) started a flood of magnetic field related models that continues today, and stimulated observational interest in the magnetic environment of flares. The prevailing concept is that a solar flare is the result of a magnetohydrodynamic (MHD) catastrophe in the corona. This MHD catastrophe leads to the reconnection of magnetic field lines in the corona that then results in a wealth of postflare phenomena (see review by Priest & Forbes 2002). The free energy that drives the flare is thought to come from currents in the corona.

To the best of our knowledge, Giovanelli (1939) was the first to search for magnetic field changes associated with flares. The development of magnetographs in the 1950s provided a new and powerful tool to study the magnetic fields associated with flares. Rust (1974) reviewed the early observations and concluded that they were unreliable because of poor sensitivity, spatial resolution, cadence, and coverage. Sakurai & Hiei (1996) reviewed more recent observations with an emphasis on the vector field measurements of two events and found that the observational picture of magnetic field changes during flares remained unclear.

With the advent of video magnetographs, some of the observational limitations of previous instruments were overcome and reports of magnetic field transients associated with the most energetic flares began to appear (e.g., Patterson & Zirin 1981). These transients were well correlated in time and location with the most intense emission of the flares. It soon became evident that these transients were the result of flare-induced line profile changes and did not indicate real changes in the magnetic field (Patterson 1984; Harvey 1986; Qiu & Gary 2003). Positive and negative reports of magnetic field changes continued through the 1980s and 1990s, leaving the observational picture confused.

During the past six years, however, much of the confusion has receded as high-quality, high-cadence observations have provided mounting evidence of rapid, permanent changes in the longitudinal and transverse magnetic fields during solar flares. Comparing preflare and postflare images from the Big Bear Solar Observatory (BBSO) video magnetograph, Cameron & Sammis (1999) detected a significant change in the longitudinal magnetic field in the active region that produced the X9.3 flare on 1990 May 24. Because this flare occurred near the limb, the observed change in the longitudinal magnetic field could be interpreted as a change in the horizontal field. Using high-cadence Michelson Doppler Imager (MDI) magnetograms of the X1 flare on 1998 May 2, Kosovichev & Zharkova (1999) detected a permanent change in the longitudinal magnetic field of about 100 G on a timescale of 1–5 minutes and on a spatial scale of 5–20 Mm. Kosovichev & Zharkova (2001) later reported on changes in the magnetic field seen at seven locations in the active region that produced the X5.2 flare on 2000 July 14. One of these regions shows a convincing case of an abrupt and persistent change in the field. The change in the field has a magnitude of $\sim$30 G and occurs on a timescale of $\sim$10 minutes.

Wang et al. (2002b) reviewed BBSO vector magnetograph data and MDI data for six X-class flares that occurred on 1991 March 22, 2001 April 2, 2001 April 6, 2001 August 25, 2001 October 19, and 2001 October 22. For all six events, they detected a permanent increase in the magnetic flux of the leading polarity of $\sim 10^{20}$ Mx and a decrease in the following polarity of lower magnitude. The timescales for these changes ranged between 10 and 100 minutes. Wang et al. (2002a) also studied the

magnetic field changes associated with an M2.4 flare that occurred on 2002 February 20. They found that a large reduction in the magnetic flux occurred during the flare and that the small sunspot where the change in the flux occurred had vanished.

Using BBSO vector magnetograph images, Spirock et al. (2002) detected a 6×10^{20} Mx increase in the positive flux in the active region that produced the X20 flare on 2001 April 2. Using MDI data, Meunier & Kosovichev (2003) found an abrupt increase in positive flux on the order of 2.0×10^{20} Mx during the X4.0 flare on 2000 November 26. Using both MDI and BBSO data, Yurchyshyn et al. (2004) detected a decrease in positive flux of 1.0×10^{20} Mx during the X4.8 flare on 2002 July 23. Using BBSO, MDI, *TRACE*, and *Reuven Ramaty High-Energy Solar Spectroscopic Imager* (*RHESSI*) data, Wang et al. (2004b) detected an increase in both the longitudinal and transverse fields on the order of several times 10^{20} Mx and on timescales of tens of minutes during the M8.7 flare on 2002 July 26. They further showed that the increase in the longitudinal component appeared at one of the footpoints of the flare, whereas the increase in the transverse field occurred between the footpoints.

Wang et al. (2004a) showed that the penumbrae close to three X-class flares on 2000 June 6, 2003 October 28, and 2003 October 29 vanished rapidly at the times of the flares. Liu et al. (2005) extended this work and included magnetic field change measurements for six X-class flares and one M-class flare. They found seven regions where a decrease in the longitudinal magnetic flux occurred and five where an increase occurred. Deng et al. (2005) did a more thorough study of penumbral and field changes with the X-class flare on 2000 June 6 and suggested that the observed changes were consistent with the outward eruption of magnetic flux above the active region. Both Liu et al. (2003) and Li et al. (2005b) studied the X3 flare that occurred on 2002 July 15. Li et al. disagreed with the suggestion of Liu et al. that the rapid changes in the magnetic field triggered the flare, noting that the field changes occurred too late to be a trigger. Li et al. (2005a) found striking changes in the positive and negative fluxes near a small sunspot during the M6.7 flare on 2001 March 10. Wang et al. (2005) reevaluated observations of the X5.7 flare on 2000 July 14 and confirmed that changes in the penumbra, the magnetic field, and the Evershed velocities occurred at the time of the flare.

All told, persistent changes in the magnetic field associated with solar flares have been reported for at least 20 flares in 14 publications during the past six years. The data sets, the data reduction techniques, and the data analysis techniques have been inhomogeneous, however, and many interpretations have been offered to explain the observed phenomena. Nonetheless, abrupt and persistent changes in the longitudinal and transverse fields do occur during X- and M-class solar flares, and the rising number of observations suggests that this might be a common phenomenon.

We have conducted a survey of X-class solar flares to search for and characterize these abrupt and persistent changes in the magnetic field. Our results are drawn from a single, homogenous data set (GONG magnetograms), using consistent data reduction and analysis techniques. The data set covers 15 X-class solar flares, 10 of which have not been in previous studies. Our goal in this paper is to characterize the changes in the longitudinal magnetic field during solar flares, not to explain the underlying cause of solar flares or to test any particular theory regarding the cause of solar flares. We do offer some discussion of several hypotheses for the cause of the observed magnetic field changes in § 5. At the conclusion of the paper, we state the most critical results from our research that any solar flare model must explain. Some of this material has been reported elsewhere in preliminary form (Sudol et al. 2004; Sudol & Harvey 2004). The results and discussion in this paper supersede our previous work.

2. DATA

Prior observations of the abrupt and persistent changes in the magnetic field during solar flares have established that the timescale for these changes is on the order of 10 minutes. Transients due to photospheric line profile changes rise and fall on timescales of a few minutes, and the magnetic field in an active region can evolve as fast as a few gauss per minute. So about an hour's worth of high-sensitivity, high-cadence data are needed to distinguish between transients, normal field evolution, and the abrupt and persistent changes in the magnetic field that have been reported to be associated with solar flares.

The GONG instruments were designed to produce full-disk images of the relative Doppler shift of the Ni I line at 676.8 nm once per minute. The difference between interleaved observations in right- and left-circularly polarized light during each minute of integration permit a measurement of the longitudinal magnetic field strength with a typical instrumental sensitivity of $\sim$3 G pixel^{-1}. The spatial scale of the GONG images is $2\farcs5$ pixel^{-1}. Six stations worldwide provide continuous coverage of the solar disk, weather permitting. The GONG magnetograms therefore provide the magnetic sensitivity, high cadence, spatial resolution, and spatial and temporal coverage required for the study of magnetic field changes during flares. As with all magnetographs, the GONG measurements of the longitudinal magnetic field are sensitive to changes in the photospheric line profile during the intense heating phase of solar flares (Ding et al. 2002; Edelman et al. 2004).

The most noticeable changes in magnetic field are expected to occur during the most energetic flares. A total of 52 X-class flares occurred from 2001 April, the start of an upgrade of the GONG instruments to a spatial scale of $2\farcs5$ pixel^{-1} and full-time magnetic field measurements, to 2003 December, the start of this project. We limited our survey to those flares for which GONG magnetograms are available under good seeing conditions from a single site for at least 1 hr before and after the flare. We eliminated from consideration all events with an apparent central meridian longitude difference greater than 65° ($\mu \approx 0.42$). The dates, times, and relevant characteristics of the 15 solar flares selected for this survey appear in Table 1.

3. DATA PROCESSING

We remapped the active region associated with each flare from the full-disk GONG magnetograms to an overhead, azimuthal-equidistant projection, $32^\circ\times32^\circ$ field of view (256×256 pixels, $0\fdg125$ pixel^{-1}) tangent to a point near the reported position of the flare. At disk center, the full-disk magnetogram scale of $2\farcs5$ pixel^{-1} in equatorial coordinates is nearly equal to the remapped magnetogram scale of $0\fdg125$ pixel^{-1} in heliographic coordinates. The remapping algorithm corrects for differential rotation and interpolates pixel values using a fourth order spline function. The maximum departure from equal area pixels is less than 2% in the corners of the remapped area.

We registered the remapped magnetograms to a 10 minute average of magnetograms prior to the flare. The registration provides a first-order correction for any drift of the active region with respect to the heliographic center of the frame and for any residual error in the orientation of solar north in the full-disk magnetograms. The shifts required to register each frame are based on a minimization of the difference between the square root of the absolute value of the frame and the square root of the

TABLE 1
FLARES STUDIED IN THIS SURVEY

Date (UT)	*GOES* Start Time	*GOES* Class	Location	NOAA Number
2001 Apr 2	2132	X20	N18W65	9393
2001 Jun 23	0402	X1.2	N10E23	9511
2001 Aug 25	1623	X5.3	S17E34	9591
2001 Oct 19	1613	X1.6	N15W29	9661
2001 Oct 22	1744	X1.2	S18E16	9672
2001 Dec 11	0758	X2.8	N16E41	9733
2002 May 20	1521	X2.1	S21E65	9961
2002 Aug 21	0528	X1.0	S12W51	10069
2003 May 27	2256	X1.3	S07W17	10365
2003 May 28	0017	X3.6	S06W25	10365
2003 Jun 10	2319	X1.3	N10W40	10375
2003 Jun 11	2001	X1.6	N14W57	10375
2003 Oct 26	0557	X1.2	S15E43	10486
2003 Oct 29	2037	X10	S15W02	10486
2003 Nov 2	1703	X8.3	S14W56	10486

absolute value of the reference frame. Because seeing-induced noise is proportional to the signal, the noise in regions of strong magnetic field can have a detrimental influence on the registration. Using the square root of the absolute value of a frame in the minimization gives higher weight to the extended, weaker fields. We estimate that the systematic residual motion of features in the registered frames is less than 1.0 pixel over 4 hr. Distortion of the images due to seeing is negligible due to the long integration time (one minute), but seeing does introduce noise where the intensity gradients and magnetic field gradients are steep.

After remapping and registering the magnetograms, we created time variation plots for all the pixels in each field of view for up to 4 hr, 2 hr on either side of the time of the peak of the flare, as indicated by the *Geostationary Operational Environmental*

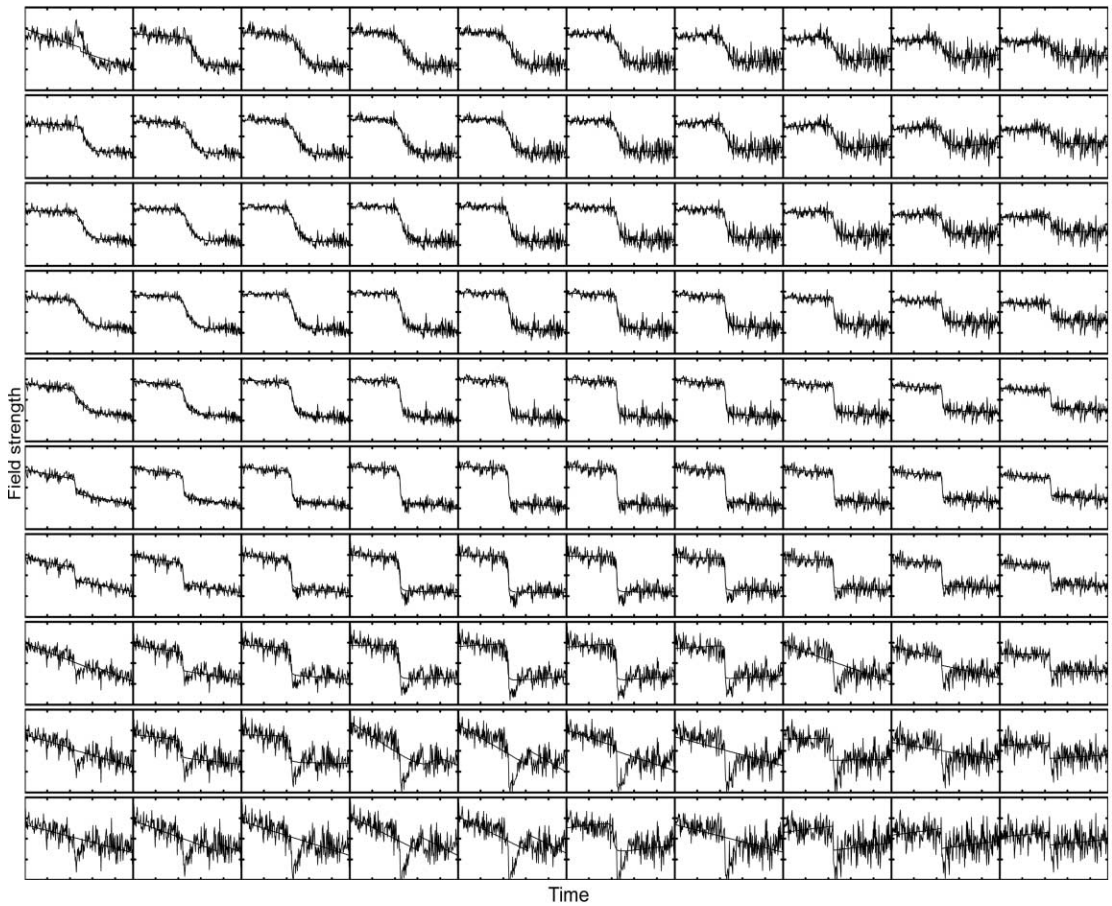

FIG. 1.—Mosaic of the time variation plots of the longitudinal magnetic field strength for a section of the active region that produced the flare on 2003 November 2. Each plot corresponds to a single pixel, and the plots cover a contiguous 10×10 pixel region. The vertical axis spans 500 G. The mean value of the magnetic field has been subtracted from the data in each plot. The horizontal axis spans 240 minutes. The fit of a step function appears plotted over the data (see text for details).

Satellite (*GOES*) 1–8 Å soft X-ray flux. In three cases, observations begin or end less than 2 hr from the peak of the flare. In these three cases, the time variation plots include all of the data available. The pixel values in the GONG magnetograms are given in units of meters per second. We have converted the pixel values to units of gauss using the scaling of 0.352 G m^{-1} s^{-1}.

From an initial investigation of the data (Sudol & Harvey 2004), we know that the time variation of the magnetic field that occurs during a flare can be characterized to first order with a step function. In order to locate all of the relevant field changes in the data, as well as to characterize the field changes, we fit a step function of the following form to all of the time variation plots at each pixel:

$$B(t) = a + bt + c\left\{1 + \frac{2}{\pi}\tan^{-1}[n(t - t_0)]\right\}, \qquad (1)$$

where a and b account for the strength and the evolution of the background field, t represents time, c represents the half-amplitude of the step, n is the inverse of the time interval controlling the slope of the step, and t_0 is the time corresponding to the midpoint of the step. The parameters a, b, c, n, and t_0 are the free parameters of the fit. The amplitude of the step, $2c$, is a measure of the change in the magnetic field, dB. The quantity πn^{-1} is a measure of the period of time over which the magnetic field change occurs, dt. (This follows from the time derivative of eq. [1], dB/dt, evaluated at $t = t_0$.) The ratio of the amplitude of the change in the magnetic field, $2c = dB$, to the period of time over which the magnetic field change occurs, $\pi n^{-1} = dt$, is a measure of the rate of change in the magnetic field, dB/dt. The first derivatives of equation (1) have a pleasing symmetry to which we attribute the stability of the fitting algorithm. We used the Levenberg-Marquardt method of nonlinear least-squares minimization to fit equation (1) to the data.

We must emphasize that equation (1) does not represent a physical model from which we can extract physical quantities. At best, in fitting equation (1) to the data, we can account for the offset and the slope in the data and therefore arrive at fair estimates of dB and dt. Even then, because the characteristic timescales of the magnetic field changes are fast compared to the cadence of our data, the fit does not result in a particularly accurate measure of the rate of change in the magnetic field. Furthermore, the fit does not take into account either slow nonlinear evolution of the magnetic field or fast transients due to line profile changes, both of which can influence the fit. Figure 1 shows the fit of equation (1) to the time variation in the longitudinal magnetic field for a 10×10 grid of pixels. Note that the field change is obvious in almost all of the pixels. The fits to the data are quite good in the top seven rows, but the fits in the bottom three rows often fail because of the transients caused by flare-induced line profile changes. The noise level, due almost entirely to seeing variations, depends on the local intensity gradients and magnetic field gradients.

From the fit parameters, we created "parameter maps," in other words, images of the fit parameters to the time variation in the longitudinal magnetic field at each pixel. Our fitting algorithm expects to find a step in the data, so normal field evolution, transients due to flare emission in the Ni I line profile, and noise can sometimes confuse the algorithm. As a consequence, sometimes we see "false" signatures of magnetic field change and bad fits, as in the bottom part of Figure 1. To eliminate these false signatures and bad fits in the parameter maps, we imposed some selection criteria when creating the parameter maps. We set all of the parameters of a fit to zero if the magnetic field change was unreasonable ($|2c| > 400$ G), if the magnetic field change occurred over too long a period of time ($n^{-1} > 20$ minutes), or if the time at which the step occurred was not within 10 minutes of the time of flare maximum ($t_0 \pm 10$ minutes). In a small number of cases, we relaxed one or more of these criteria if we had sufficient evidence to do so. Figure 2 shows one example of these parameter maps for the flare on 2003 November 2. Gray areas in the left panels (black areas in the right panels) are locations where at least one fit parameter lies outside our selection criteria. In this example, the a and c maps are almost inverses of each other indicating that the line-of-sight component became weaker during the flare. The n^{-1} map indicates that the timescale for the magnetic field change was about the same throughout the active region. The t_0 map shows some variation, indicating that the magnetic field changes did not occur at the same time across the active region, or within the areas where field changes occurred, a topic that we discuss further in § 4.4. The σ^2 map represents the scatter in the data with respect to the fit. The scatter increases in regions of higher magnetic field strength, so there is a high correlation between a and σ^2.

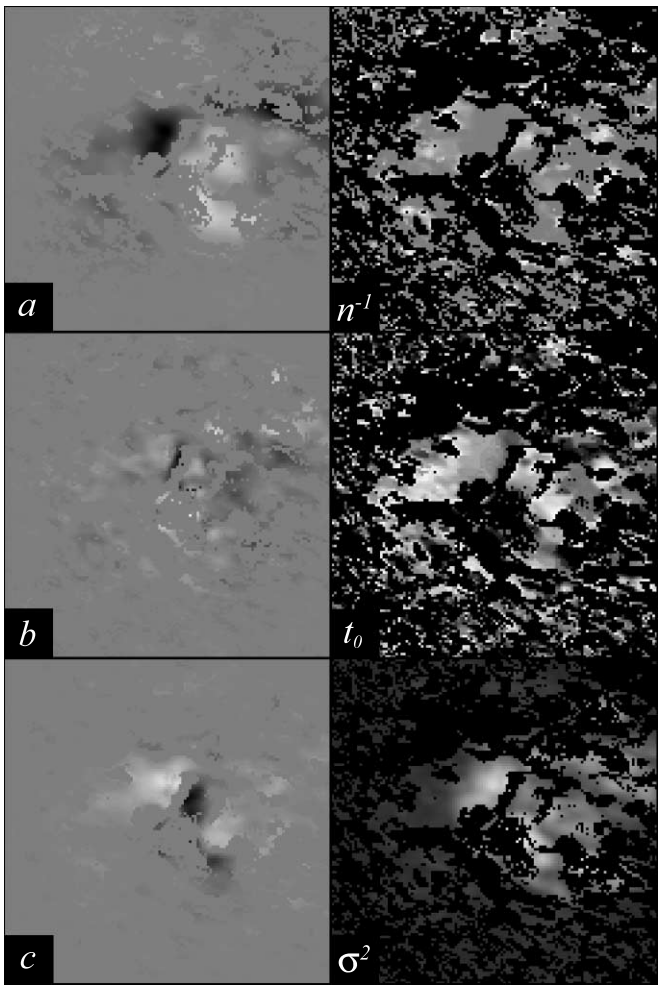

FIG. 2.—"Parameter maps," cropped to 128×128 pixels, for the active region that produced the flare on 2003 November 2. The fit parameters a, b, and c appear in the left column from top to bottom, respectively. The fit parameters n^{-1} and t_0 and the scatter of the data with respect to the fit, σ^2, appear in the right column from top to bottom, respectively. In both columns, the images are stretched so that the full range of values is represented from black to white. In the left column, gray represents excluded data. In the right column, black represents excluded data.

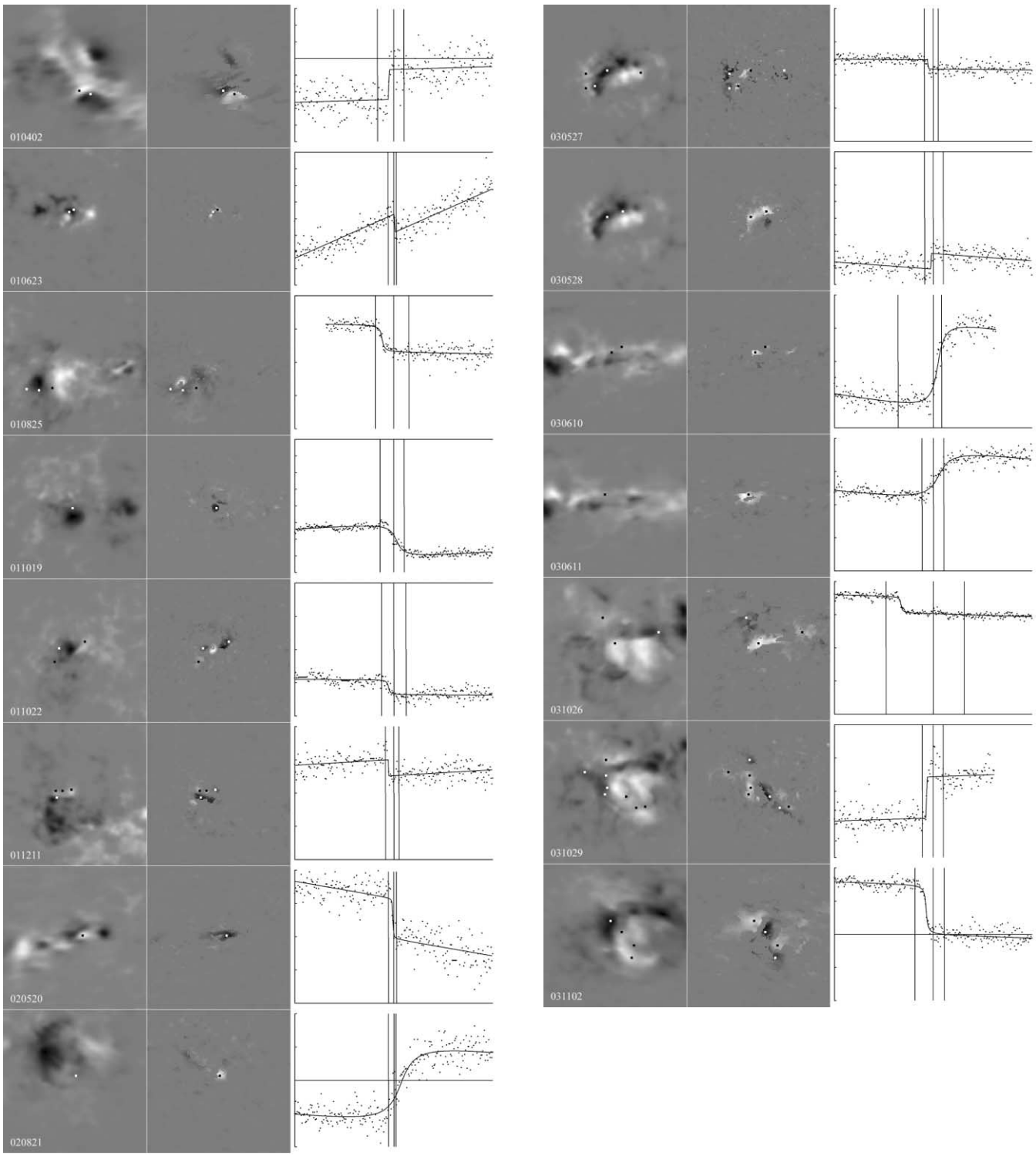

FIG. 3.—Observational synopsis of the 15 flares in this survey. *Left column*: Remapped, 128×128 pixel image of a 10 minute average of the longitudinal magnetic field in the flaring active region prior to the flare. *Middle column*: A 128×128 pixel *dB* map for the active region in the left column. In the left and middle columns, representative points are marked with boxes. The shading of the box is chosen to create the highest contrast against the background and is not significant. *Right column*: Time variation plot of the longitudinal magnetic field for one of the representative points. A fit to the data is plotted as well. The three vertical bars denote the time of the start, peak, and end of the flare according to the *GOES* X-ray flux. The vertical axis spans either 400 or 800 G. Tick marks appear at intervals of 100 G, and the zero field line is included in all plots. The horizontal axis spans 240 minutes, centered on the time of the peak of the flare. The date of the flare is given in the bottom left corner in the left frame in a six-digit representation (yymmdd).

The maps of the change in the magnetic field, which we refer to as "*dB* maps," have served as a guide for us in locating those areas of the active region where a significant change in the magnetic field near the time of the flare has occurred. Because of the confusion caused by normal field evolution, transients, and noise, and because of the exclusion of some of the fits in creating the parameter maps, the parameter maps are sometimes incomplete in that they do not necessarily show the entire region where an abrupt and persistent change in the magnetic field has occurred. The reader should be careful not to overinterpret these maps. To

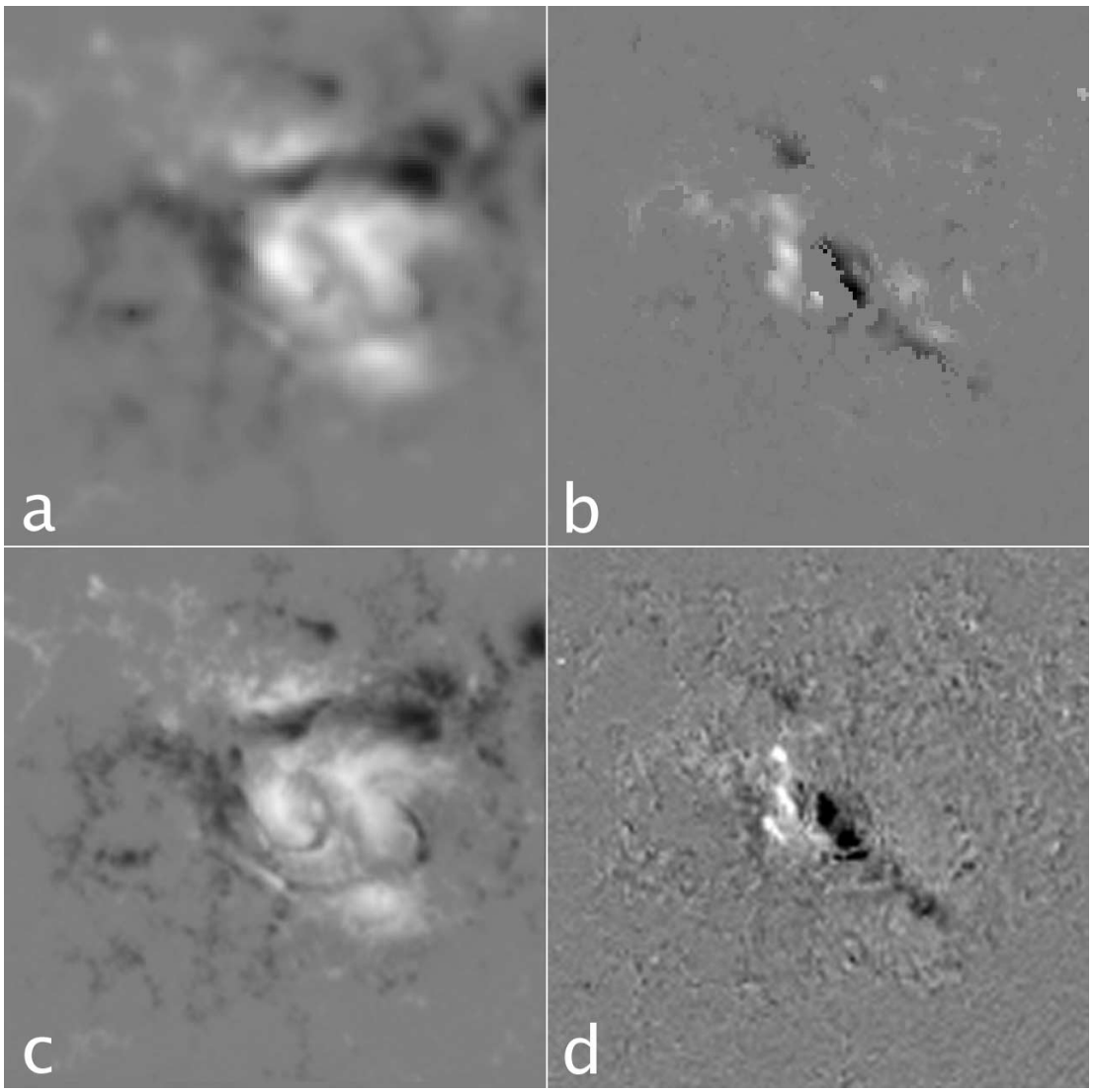

FIG. 4.—Comparison of GONG and MDI data for the flare on 2003 October 29. (*a*) A 10 minute average of GONG magnetograms just prior to the flare. (*b*) A *dB* map from the GONG data. Note that the central area is blank where magnetic transients prevented fitting by eq. (1). (*c*) A 10 minute average of MDI magnetograms just prior to the flare. (*d*) Difference between 10 minute averages of MDI magnetograms taken 10 minutes prior to the start of the flare and 10 minutes after the start of the flare. The MDI and GONG results are nearly identical except for the difference in spatial resolution and the data excluded from the *dB* map.

aid our own interpretation of such regions, we also prepared maps (not shown) of the difference between a 10 minute average of the field prior to the time of the change in the magnetic field and a 10 minute average 1 hr after the field change.

To distinguish the abrupt field changes associated with flares from false signatures in the *dB* maps, we reviewed by eye the time variation plots and the fits to those plots for each pixel in one or more regions of interest selected from the *dB* maps. To deal with the high volume of data, we produced single-frame, 10×10 grids of the time variation plots, allowing us to review 100 plots at once, as in Figure 1. Overall, we reviewed more than 8000 plots. From this review, we selected a "representative point" for each area where an abrupt and significant field change occurred. We selected 42 points in all. These representative points are averages of 4 pixels that approximate the most abrupt and the most significant change in the magnetic field. We have combined 4 adjacent pixels because the average resolution in the GONG magnetograms is $\sim 5''$, so an average of 4 pixels better represents the true resolution of the data.

We must emphasize that we have selected these representative points by inspection, so these points are not necessarily the most abrupt and the most significant points, but approximately so. We have taken this approach in order to avoid the effects of averaging transients and normal field evolution into a measurement of the change in the magnetic field over a large region.

In Figure 3, we present remapped images of the average magnetic field prior to the flare for the 15 active regions in our survey. We present *dB* maps for each active region, and we mark all of the representative points that we have used in our analysis. We also include the time variation plot and the fit of equation (1) to that plot for one of the representative points in each active region in order to illustrate the characteristics of the field changes. The vertical lines denote the start, peak, and end times of the flare according to the *GOES* 1–8 Å soft X-ray flux. We note at once that the fields do not change before the start of the flares. In most cases, the field changes are complete before the end of the flare, and often before the peak of the flare.

In Figure 4, we demonstrate that GONG and MDI data show similar magnetic field changes despite the differences in the instruments and observational techniques. In seeking comparable data, we found that MDI observations at a 1 minute cadence were not available for most of the flares in our survey. The best

observed case is the flare on 2003 October 29. In Figure 4, we compare GONG data (*top row*) to MDI data (*bottom row*) for this flare. We have remapped the MDI magnetograms in the same manner as the GONG magnetograms and to the same scale. Figures 4*a* and 4*c* show 10 minute averages of the GONG and MDI magnetograms, respectively, prior to the flare. Figure 4*b* shows the *dB* map from Figure 3. Figure 4*d* shows the difference between a 10 minute average of the MDI magnetograms 10 minutes after the start of the flare and Figure 4*c*. This difference image is nearly identical to the *dB* map, except for the differences in spatial resolution and the data excluded from the *dB* map. This bolsters confidence in the data from both instruments and the results presented here.

4. ANALYSIS

In this section, we discuss the characteristics of the representative points selected as described in § 3. We compare the GONG data to other data, and we discuss some cases in which the change in the magnetic field appears to propagate across the active region.

4.1. *General Characteristics of the Field Changes*

During all 15 X-class solar flares in our survey, the longitudinal magnetic field in at least one location in the flaring active region undergoes an abrupt, significant, and permanent change. Using the fits of equation (1) to the representative points, we can quantify abrupt to mean that the time over which the magnetic field change occurred, πn^{-1}, is typically less than $\sim$10 minutes as shown in the distribution function in Figure 5. Almost half of the magnetic field changes are unresolved at a one-minute cadence. We must caution the reader that the time over which the magnetic field change occurred might be biased in some cases to a shorter value due to a transient and in other cases to a longer value because the cadence of the observations is 1 minute. Regardless, it is apparent from Figure 3 that the field changes are in general abrupt.

The amplitudes of the field changes reported here are at least 1.4 times, and as high as $\sim$20 times, the standard deviation of the noise in the preflare field as shown in the distribution function in Figure 6. Given that most field changes occur in less than 10 minutes and are not much greater than the noise in amplitude, it is not surprising that so much confusion about magnetic field changes has persisted for so long. These results also suggest that fast, small-amplitude changes are frequent but have largely gone unobserved.

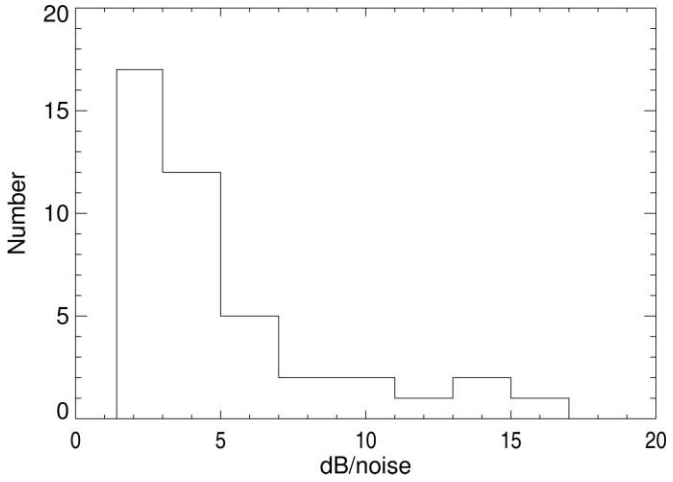

FIG. 6.—Distribution of the significance of the change in the magnetic field, defined to be the ratio of the amplitude of the change in the field, *dB*, to the rms scatter of the data with respect to the fit prior to the change in the magnetic field.

In all cases, the observed field change persists until the end of the data run, which is in most cases 2 hr past the peak of the flare (see Figs. 1 and 3). As mentioned before, in three cases, the GONG instrument unstowed or stowed within the 4 hr window around the time of the peak of the flare that we have imposed on the data. In two of these cases, 2003 June 10 and 2003 October 29, the instrument stowed. In these two cases, the field changes persist for 74 and 76 minutes, respectively. The differences are hardly worth noting, and for all intents and purposes, the field changes are "permanent."

To emphasize this point, our longest, single-site magnetogram sequences, extending for more than 5 hr after the flares on 2001 August 25 and 2002 May 20, show no indications of a return to preflare conditions, only slow, evolutionary changes of a much lower amplitude than the abrupt changes during the flare.

In Figure 7, we present a plot of the magnetic field against the change in the magnetic field, *B* versus *dB*, for all of the representative points. There is no apparent correlation between the magnitude of the magnetic

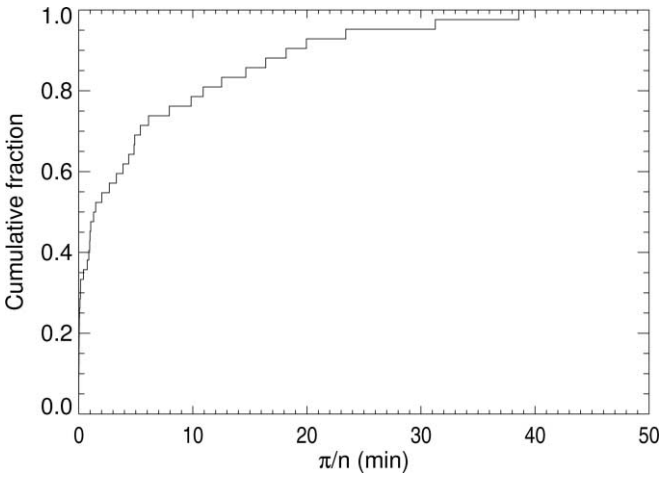

FIG. 5.—Cumulative histogram of the time over which the magnetic field change occurred, πn^{-1}.

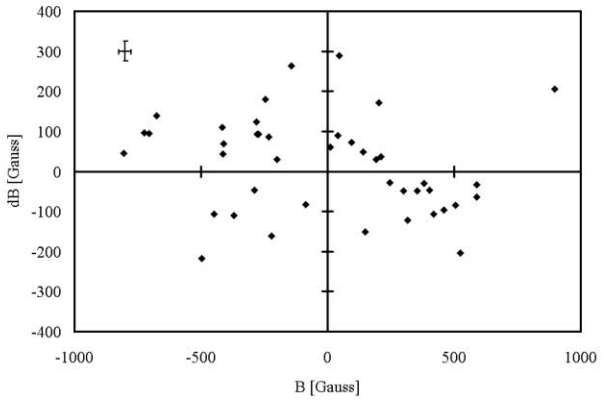

FIG. 7.—Plot of the longitudinal magnetic field, *B*, prior to the flare, against the change in the field, *dB*, during the flare. Representative error bars are given in the top left corner.

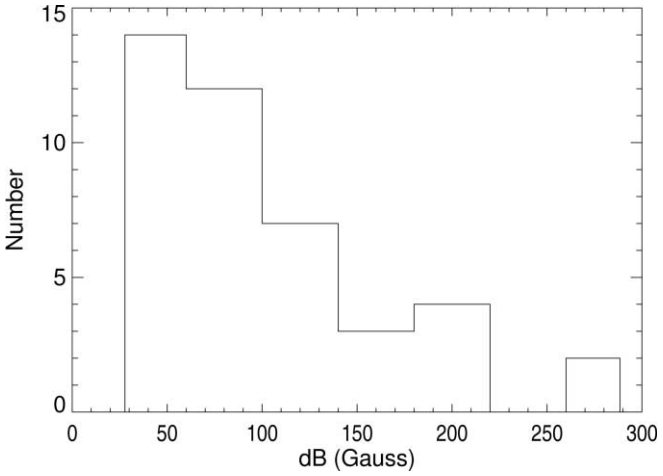

FIG. 8.—Distribution of the absolute value of the change in the magnetic field, $|dB|$.

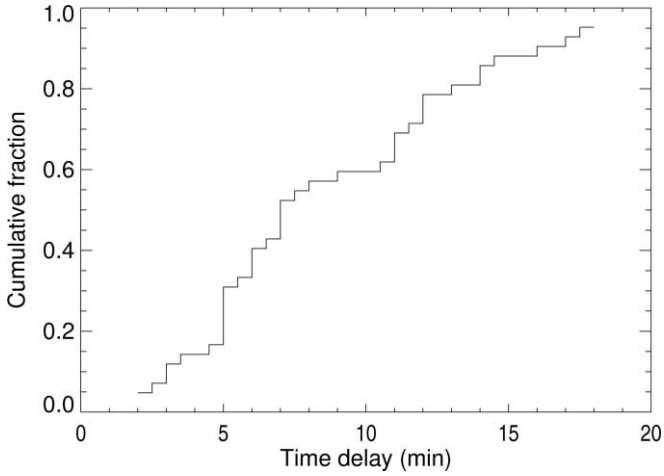

FIG. 9.—Cumulative histogram of the difference between the time at which the field change occurred and the time of the start of the X-ray flare.

field change. No trends appear when we sort the data by hemisphere or by distance from the disk center. The majority of the field changes occur in regions where the field strengths are on the order of hundreds of gauss, which suggests locations close to or within sunspots, given the resolution of the data. Changes that reduce the measured field component are about twice as common as those that increase it, and changes that result in a switch in the polarity of the field are rare, occurring in just two cases.

Wang et al. (2002b) noted that during all six events in their survey, the leading flux always increased, whereas the following flux tended to decrease and by a smaller amount. It is difficult for us to comment on this observation because in some cases we see a field change at only one location. In other cases, we see multiple sites of field change, and it is often difficult to determine which flux would constitute the leading flux in complex active regions.

The distribution of the changes in the magnetic field, dB, is shown in Figure 8. The notch in the histogram near zero is a consequence of the noise, which is typically $\sim$20 G. The histogram of field changes suggests that small-amplitude changes are more numerous but go unobserved, being buried in the noise in the data. In our sample, the weakest observed field change is 28 G, the strongest, 288 G. The median of the absolute values of the field changes is 90 G.

To calculate the rate of change in the field, dB/dt, we have divided $2c$ by πn^{-1}, replacing πn^{-1} with 1.0 if $\pi n^{-1} < 1.0$. We have made this substitution because the cadence of our data is 1 minute, so we know that we cannot determine the time over which the change in the magnetic field occurs to better than 1 minute. The rates of change in the magnetic field range between 2 and 200 G minute^{-1}, with majority being between 2 and 40 G minute^{-1}. We must emphasize that these are rough estimates, and the most conservative conclusion would be that the rates of change in the field are on the order of tens of gauss per minute, and perhaps as high as 200 G minute^{-1}.

Aside from establishing the basic characteristics of the magnetic field changes, we can also establish when the magnetic field changes occur relative to the start of the flare, which is critical to understanding the cause and effect relationships between flare phenomena. None of the examples in Figure 3 show a clear change in the magnetic field before the start of the X-ray flare. Figure 9 extends this result to all of the representative points. Figure 9 shows the cumulative histogram of the difference between the time of the start of the change in the magnetic field, which we have taken to be $t_0 - 0.5\pi n^{-1}$, and the time of the start of the X-ray flare. In one case, 2002 August 21, the difference is negative, indicating that the magnetic field change occurred before the X-ray flare. We do not consider this one case to be significant, and we expect that n^{-1} is biased to a higher value because of the noise in the data. These statistics suggest that the photospheric magnetic field changes are a consequence of some other event that triggers the flare, not the trigger itself.

The results that we have presented so far suggest that the changes in the magnetic field are not systematic. It is possible, though, that a change in the vector field (its tilt with respect to the line of sight), the change in the flux, or the total change in the magnetic energy are much more important physical quantities than those that we have presented here. For example, there could be a correlation between the change in the tilt of the field and the energy released during the flare, but due to the limited aspect of our observations, only a fraction of the field change is observed. We note, however, that there is no detectable correlation between the magnitude of the change in the field and the heliocentric angle, ρ. We do not have vector field data, and we cannot make an accurate measurement of the change in the total flux or the magnetic energy in the region because of the confusion caused by normal field evolution and transients.

Finally, we must emphasize that we have arrived at our measurements of the changes in the magnetic field in the smallest resolution elements at those locations where approximately the most abrupt and the most significant changes in the magnetic field have occurred. Changes in the magnetic field are present over as much as $\sim 2^\circ$ of the surface in some events. The magnitude of the change in the field in general decreases from a central maximum (near the representative point), and the rate of change can be quite variable, often blending into what appears to be normal field evolution, as can be seen in Figure 1.

4.2. *Location of Field Changes*

In addition to remapping the GONG magnetograms, we have remapped a GONG "white light" image for each flare (Fig. 10). Superimposing the representative points on the white light images, we find that the majority of the field changes occur in the penumbrae of sunspots. Only in three cases do we observe field changes occurring clearly within the umbra of a sunspot. We should note, however, that the magnetic field within the umbra

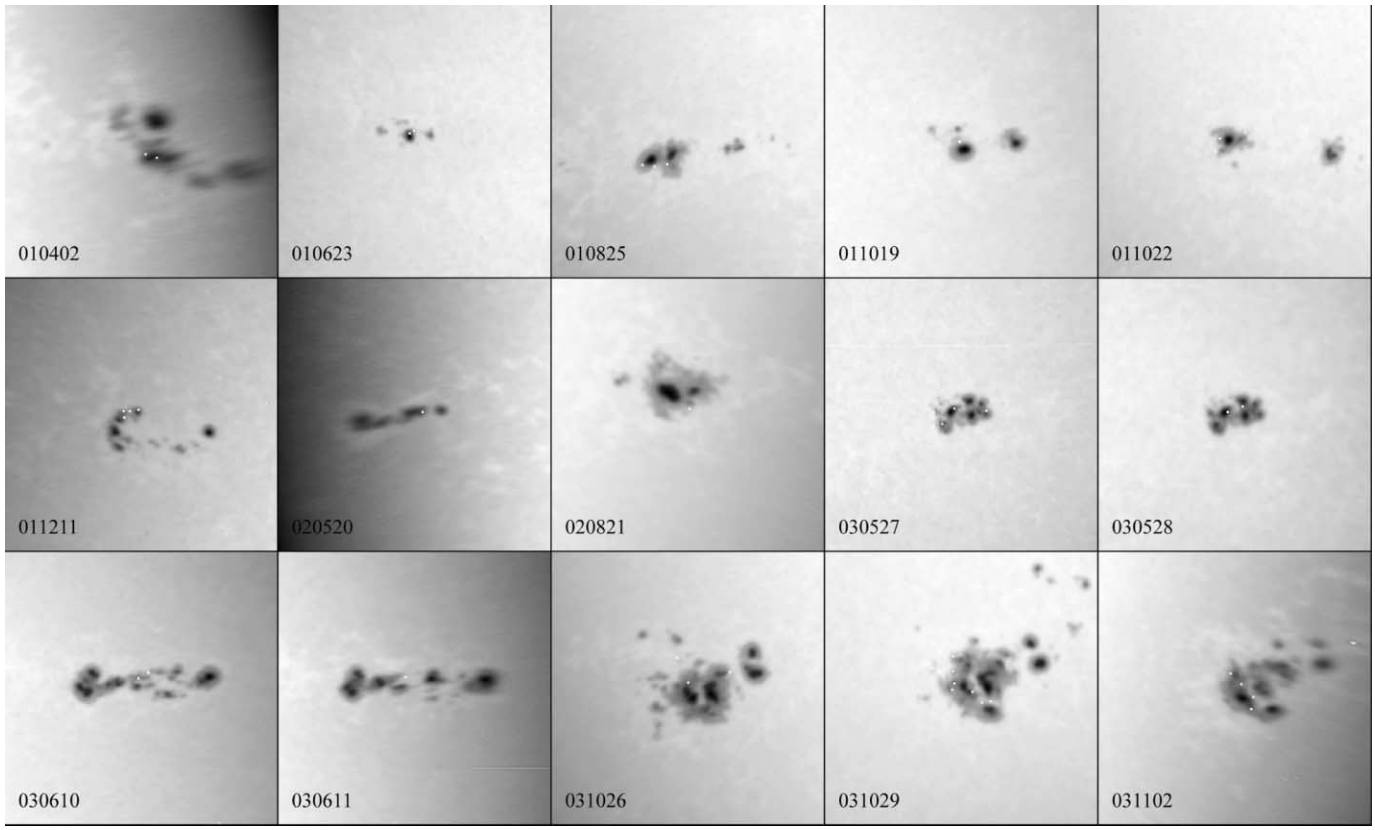

FIG. 10.—GONG "white light" images for each active region, remapped to the same time and coordinates as the magnetograms. The representative points are marked with white boxes. Note that almost all of the field changes occur in the penumbrae of sunspots.

is quite strong, so the noise is quite high, so some field changes within the umbrae might have gone unobserved. The dark background of the umbra also makes it more probable for flare-induced line profile emission transients to be present in the data. These regions tend to be excluded in our analysis because of the effect of the transient on the fit to the data.

Rapid penumbral decay during several X-class and M-class flares was first noted by Howard (1963) and later observed by Liu et al. (2005), Deng et al. (2005), and Wang et al. (2004a, 2005). In particular, Liu et al. (2005) have reported a roughly equal mix of increasing and decreasing longitudinal magnetic flux in the regions of penumbral decay, consistent with our results. The correlation between penumbral decay and longitudinal magnetic field changes is tantalizing, but we cannot say anything more about the connection between these phenomena with our data.

4.3. *Comparison with Flare Emission*

TRACE images at 1600 Å are available at the time of the flare for eight of the flares in our survey, but "complete" series of high-cadence images before, during, and after the flare are available for only three events: 2001 August 25, 2003 October 26, and 2003 October 29. We selected *TRACE* images at a two-minute cadence for up to 30 minutes prior to the flare and for 60 minutes after the flare, and some additional images at 90, 120, 150, and 180 minutes after the flare, if available. We remapped these images to the same coordinates as the GONG magnetograms. We then registered the *TRACE* images to the GONG magnetograms if needed. The registration is good to a couple of pixels, and the reader must keep in mind that the *TRACE* features are above the photosphere whereas GONG magnetograms reveal magnetic field structure within the photosphere.

In the three cases for which we have a series of *TRACE* images, we see excellent spatial and temporal correlation between the representative points in the GONG magnetograms and bright features in the *TRACE* images. In the same location, to within $0^{\circ}.5$ in heliographic coordinates, and at the same time, to within 4 minutes, when a change in the magnetic field occurs in the GONG magnetograms, a rapid increase in the intensity of a *TRACE* feature occurs. One example appears in Figure 11. Where magnetic field changes persist, the *TRACE* features decrease in brightness or vanish altogether after 120 minutes, indicating that the field changes are not an instrumental effect. The reverse is not true; flare ribbons in the *TRACE* images do not always correlate with detectable magnetic field changes in the GONG magnetograms. It is suggestive in Figure 11 that the time derivative of the *TRACE* light curve of the flare might correlate well with the timing of the field change. Whether this is just an insignificant coincidence would have to be tested using more data than we have available.

4.4. *Propagation of the Field Change*

In six cases, the change in the magnetic field appears to occur at progressively later times across the active region. In other words, the change in the magnetic field appears to propagate across the active region. In Figure 12, we present a section of the parameter map for t_0 for the flare on 2001 December 11 (*middle panel*). The rate of propagation between the triangular markers in Figure 12 is $\sim$5 km s^{-1}, as shown in the plot on the right (*black*

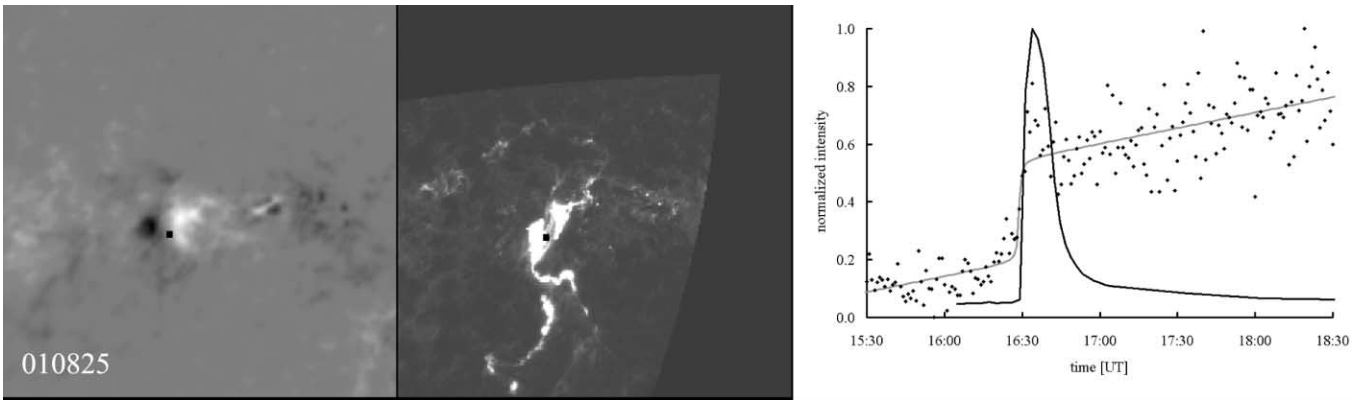

FIG. 11.—*Left*: Remapped GONG magnetogram for the flare on 2001 August 25. *Middle*: *TRACE* image at the time of the peak of the flare on 2001 August 25 remapped to the same time and coordinates as the GONG magnetogram. The black box in the GONG magnetogram and the *TRACE* image marks one of the representative points. The representative point in the *TRACE* image is double the size of the point in the magnetogram to accommodate the error in the remapping of the *TRACE* image. *Right*: Normalized time variations for the representative point in the GONG magnetogram (*gray line*) and the *TRACE* intensity image (*black line*). The data points represent the time variation in the longitudinal magnetic field as in Fig. 3.

diamonds). We have selected this particular example because it is the slowest and occurs over a large area of the surface, almost 1°, and is therefore the easiest to detect. In general, the propagation rates range between 5 and 30 km s^{-1}. Higher propagation rates are more difficult to detect; 30 km s^{-1} corresponds to about 1 pixel $minute^{-1}$ at disk center.

In the case of the flare shown in Figure 12, and given the results of the previous section, it is interesting to consider the motion of the flare ribbons. Hα images of this flare taken at Yunnan Astronomical Observatory at about a one-minute cadence are available from the Global High Resolution Hα Network; however, the images of the ribbons are saturated for several minutes around the time of maximum and their structure cannot be seen at these times. We remapped and registered the Hα images in the same manner as the *TRACE* images. The flare ribbon positions at 08:06:17 UT (*gray line*) and 08:26:46 UT (*white line*), estimated by eye, are included in the left and middle panels of Figure 12. In the right panel, we plot several measurements of the position of the southern flare ribbon (*gray squares*) along the line between the triangular markers in the middle panel. The apparent propagation of the field change and the motion of the southern flare ribbon are well correlated with a common rate of about 5 km s^{-1}. The fact that the field change propagates and that the rate of propagation is similar to that of the Hα two-ribbon flares (Švestka 1976) could be a significant clue to the origin of the field changes. Higher spatial and temporal resolution will be needed to fully exploit this association.

5. DISCUSSION

Our results show that abrupt, significant, and permanent changes of the photospheric longitudinal magnetic field are ubiquitous features of X-class flares. This means that one of the basic assumptions of modern flare theories (see Priest & Forbes 2002), that the photospheric magnetic field does not change during flares, needs to be reexamined.

We consider now what physical scenario might explain our observations. Unfortunately, our ability to discriminate among flare models is restricted because our observations are limited to the line-of-sight component of the magnetic field.

1. Horizontal mass flows might compress or diffuse the magnetic field. This seems improbable because the speeds required are approximately equal to the sound speed in the photosphere. Such mass flows would have to occur simultaneously at several

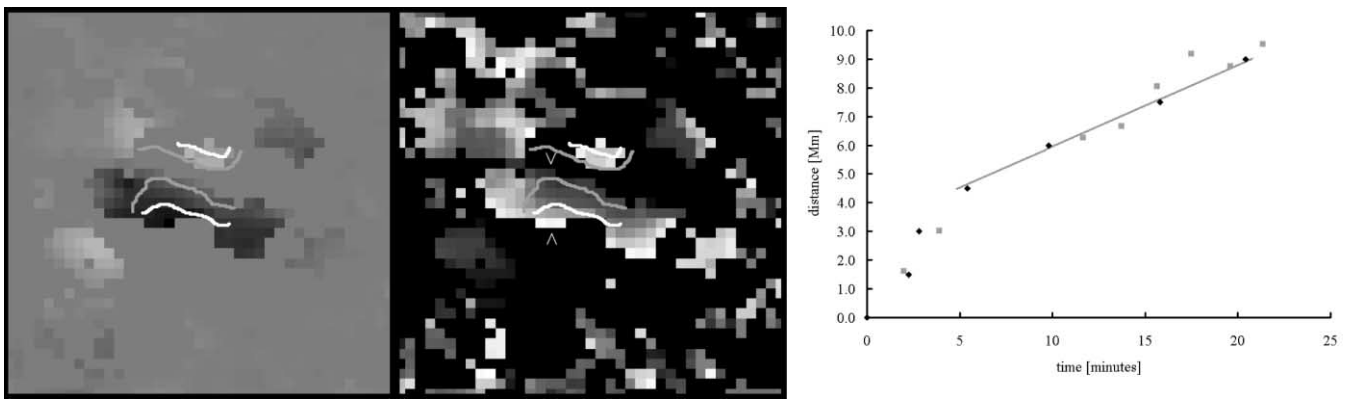

FIG. 12.—*Left*: 40×40 pixel *dB* map for the flare on 2001 December 11. *Middle*: 40×40 pixel t_0 map for the flare on 2001 December 11. Lighter shades are later in time. Overplotted on the left and middle panels are estimates of the positions of Hα flare ribbons at 08:06:17 UT (*gray*) and 08:26:46 UT (*white*). *Right*: Black diamonds indicate the times of the magnetic field change from the top triangular marker to the bottom triangular marker. The gray line indicates a propagation rate of 5 km s^{-1}. Gray squares represent measurements of the position of the southern Hα flare ribbon along the line joining the triangular markers. The uncertainty is about 1.5 Mm. The propagation rates of the magnetic field change and the flare ribbon are nearly identical at ~5 km s^{-1}.

locations in an active region, and the net flux of the region would not change, contrary to the observations (although we note the observation of high-speed flows reported by Meunier & Kosovichev 2003).

2. A portion of the existing field pattern might shift horizontally. This also seems improbable because, again, the net flux would not change.

3. A subsurface flux pattern might emerge to combine with the existing pattern. We cannot exclude this possibility, and it has the attraction of being able to explain the reversal in the polarity of the field that is sometimes observed. However, it requires impressive local flux emergence rates of the order of 10^{18} Mx s^{-1} with connectivity across a large fraction of a large active region.

4. Some of the existing flux pattern might submerge out of sight. This seems unlikely for the same reasons as item 3.

5. The current system that produces the observed field is diminished by chromospheric ablation or evaporation caused by the flare. This cannot account for cases in which the magnetic field increases in strength.

To us, the most likely explanation of the observations is that the magnetic field changes direction rather than strength, at least in the observed layer of the atmosphere. Thus, the observed longitudinal field strength might increase or decrease depending on the location of the active region on the disk and the initial orientation of the field vector relative to the observer. The close spatial association of many of the field changes with penumbrae and the recent observations that penumbrae weaken during flares suggest that the field change is such as to make the penumbral magnetic field more vertical. In other words, one viable scenario is that the field lines are pulled or relax upward by the erupting flare. Vector magnetograms taken at high cadence and with high spatial resolution should readily indicate whether or not this is the case.

At the start of this discussion we challenged one of the basic assumptions of modern flare theories. We do not mean to suggest that there is a serious flaw in these theories, however. The fact that the change in the magnetic field is delayed with respect to the start of the flare suggests that the field changes that we have observed represent yet another phenomenon among the multitude of phenomena that accompany solar flares. Yet this is not to say that the magnetic field changes are insignificant. It takes work to tilt a strong flux system at the rates suggested by the observations, and at the very least, if our favored scenario is correct, this needs to be included in the energy budget of any flare theory.

Flare models concentrate on activity in the corona, treating the photosphere as a source of energy to drive currents in the corona and generally neglecting flare-associated events in the photosphere. After surveying flare models, we have to agree with Wang et al. (2005) that we find none capable of interpreting all of the observations. The rainbow reconnection model of Somov et al. (2003) has many attractive features but needs further development. With the advent of new observations showing significant changes in the photosphere associated with flares, models should be broadened to cover a larger range of heights. While we have suggested that the observed field changes are consequences rather than triggers of the flares, that does not mean that surface or subsurface events cannot be the trigger. There is increasing evidence for a close association between specific subsurface motions and flare productivity (e.g., Komm et al. 2005), so comprehensive flare theories may need to extend from the corona to well beneath the photosphere. For example, there is evidence for the existence of subsurface vortex rings that act as a stabilizing collar around sunspots and active regions. We might speculate that a local weakening of such a ring could trigger a flare through a perturbation of the field lines connecting the solar interior to the corona. A hypothetical path connecting the interior to the corona might run along the nearly horizontal field lines (darker component) in the penumbra, couple to the less inclined field lines (brighter component) in the penumbra, and then to the corona. Similarly, the inrush of reconnecting field lines above the active region in the early stages of the flare could reduce the average inclination of field lines in the penumbra, leading to the sort of effects that we have observed. We do not want to overemphasize the possible role of the penumbra because flares occur in regions without sunspot penumbrae and we see magnetic field changes that are not associated with penumbrae. Our speculation clearly needs far more elaboration to be taken seriously and is intended only to suggest how flare models should cover a larger range of altitudes.

6. CONCLUSIONS

The most important conclusion to be drawn from the data is that abrupt, significant, and persistent changes in the longitudinal magnetic field are common during X-class solar flares. It might be the case that these magnetic field changes always occur during X-class flares, or all classes of solar flares for that matter.

Any theory that aims to explain the full range of solar flare phenomena must include the following:

1. The change in the longitudinal magnetic field typically occurs in less than 10 minutes.
2. The change in the longitudinal magnetic field is permanent.
3. The magnitude of the change in the longitudinal magnetic field, dB, at the point where the change is most abrupt and of the greatest magnitude is poorly correlated with the magnitude of the underlying field.
4. The distribution of the magnitudes of the changes in the longitudinal magnetic field at the point where the change is most abrupt and of the greatest magnitude ranges over values from 30 to 300 G, with 90 G being a typical value.
5. The rate of change in the longitudinal magnetic field, dB/dt, is on the order of tens of gauss per minute and could be as high as 200 G minute^{-1}.

Such a theory must explain the strong spatial and temporal correlation between the rapid increase in brightness at 1600 Å and the change in the longitudinal magnetic field. Such a theory must also explain the apparent propagation of the field change across as much as 1° of the solar surface at a rate of 5–30 km s^{-1} and perhaps higher. Further observations to determine the connection between the propagation of the field change and the motion of flare ribbons would perhaps go a long way to understanding the cause of the changes in the magnetic field. Finally, we urge flare theorists to increase the range of their models to include phenomena in the photosphere and below.

An obvious extension to this survey of GONG magnetograms is to include weaker flares and to relax some of the selection criteria imposed on the data in this initial survey.

This work utilizes data obtained by the Global Oscillation Network Group (GONG) Program, managed by the National Solar Observatory, which is operated by AURA, Inc., under a cooperative agreement with the National Science Foundation. The data were acquired by instruments operated by the Big Bear Solar Observatory, High Altitude Observatory, Learmonth Solar Observatory, Udaipur Solar Observatory, Instituto de

Astrofísico de Canarias, and Cerro Tololo Inter-American Observatory. We thank GONG staff members for acquiring the original data and processing it into a useful form for this project. This work uses data courtesy of the *SOHO* MDI consortium. *SOHO* is a project of international cooperation between ESA and NASA. This work uses data from the *TRACE* mission. *Transition Region and Coronal Explorer* (*TRACE*) is a mission of the Stanford-Lockheed Institute for Space Research (a joint program of the Lockheed-Martin Advanced Technology Center's Solar and Astrophysics Laboratory and Stanford's Solar Observatories Group), and part of the NASA Small Explorer Program. We acknowledge use of data from the Global High Resolution Hα Network, operated by the Big Bear Solar Observatory, New Jersey Institute of Technology, and thank Vasyl Yurchyshyn for preparing data from Yunnan Astronomical Observatory for us. We thank the referee for stimulating and constructive comments.

REFERENCES

Cameron, R., & Sammis, I. 1999, ApJ, 525, L61
Cowling, T. G. 1953, in The Sun, ed. G. P. Kuiper (Chicago: Univ. Chicago Press), 532
Deng, N., Liu, C., Yang, G., Wang, H., & Denker, C. 2005, ApJ, 623, 1195
Ding, M. D., Qiu, J., & Wang, H. 2002, ApJ, 576, L83
Edelman, F., Hill, F., Howe, R., & Komm, R. 2004, in Proc. *SOHO* 14/GONG 2004 Workshop, ed. D. Danesy (ESA SP-559; Nordwijk: ESA), 416
Giovanelli, R. G. 1939, ApJ, 89, 555
———. 1948, MNRAS, 108, 163
Gold, T., & Hoyle, F. 1960, MNRAS, 120, 89
Harvey, J. 1986, in Small-Scale Magnetic Flux Concentrations in the Solar Photosphere, ed. W. Deinzer, M. Knölker, & H. Voight (Göttingen: Vandenhoeck & Ruprecht), 25
Howard, R. 1963, ApJ, 138, 1312
Hoyle, F. 1949, Recent Researches in Solar Physics (Cambridge: Cambridge Univ. Press)
Komm, R., Howe, R., Hill, F., González Hernández, I., & Toner, C. 2005, ApJ, 631, 636
Kosovichev, A. G., & Zharkova, V. V. 1999, Sol. Phys., 190, 459
———. 2001, ApJ, 550, L105
Li, J. P., Ding, M. D., & Liu, Y. 2005a, Sol. Phys., in press
Li, J., Mickey, D. L., & LaBonte, B. J. 2005b, ApJ, 620, 1092
Liu, C., Deng, N., Liu, Y., Falconer, D., Goode, P. R., Denker, C., & Wang, H. 2005, ApJ, 622, 722
Liu, Y., Jiang, Y., Ji, H., Zhang, H., & Wang, H. 2003, ApJ, 593, L137
Meunier, N., & Kosovichev, A. 2003, A&A, 412, 541
Patterson, A. 1984, ApJ, 280, 884
Patterson, A., & Zirin, H. 1981, ApJ, 243, L99
Priest, E. R., & Forbes, T. G. 2002, A&A Rev., 10, 313
Qiu, J., & Gary, D. E. 2003, ApJ, 599, 615
Rust, D. M. 1974, in Flare Related Magnetic Field Dynamics, ed. Y. Nakagawa & D. M. Rust (Boulder: HAO/NCAR), 243
Sakurai, T., & Hiei, E. 1996, Adv. Space Res., 17(4/5), 91
Somov, B. V., Kosugi, T., Hudson, H. S., Sakao, T., & Masuda, S. 2003, Adv. Space Res., 32(12), 2439
Spirock, T. J., Yurchyshyn, V. B., & Wang, H. 2002, ApJ, 572, 1072
Sudol, J. J., & Harvey, J. W. 2004, in Proc. *SOHO* 14/GONG 2004 Workshop, ed. D. Danesy (ESA SP-559; Nordwijk: ESA), 643
Sudol, J. J., Harvey, J. W., & Howe, R. 2004, BAAS, 36, 714
Švestka, Z. 1976, Solar Flares (Dordrecht: Reidel)
Wang, H., Ji, H., Schmahl, E. J., Qiu, J., Liu, C., & Deng, N. 2002a, ApJ, 580, L177
Wang, H., Liu, C., Deng, Y., & Zhang, H. 2005, ApJ, 627, 1031
Wang, H., Liu, C., Qiu, J., Deng, N., Goode, P. R., & Denker, C. 2004a, ApJ, 601, L195
Wang, H., Qiu, J., Jing, J., Spirock, T. J., Yurchyshyn, V., Abramenko, V., Ji, H., & Goode, P. R. 2004b, ApJ, 605, 931
Wang, H., Spirock, T. J., Qiu, J., Ji, H., Yurchyshyn, V., Moon, Y.-J., Denker, C., & Goode, P. R. 2002b, ApJ, 576, 497
Yurchyshyn, V., Wang, H., Abramenko, V., Spirock, T. J., & Krucker, S. 2004, ApJ, 605, 546